

Astronomical Notes

Astronomische Nachrichten

Hopf bifurcations with fluctuating gain

S.A. Triana¹, D.H. Kelley¹, D. Zimmerman¹, D. Sisan², and D.P. Lathrop^{1,3}

¹ Department of Physics and Institute for Research in Electronics & Applied Physics, University of Maryland, College Park, MD 20742, USA

² Department of Physics, Georgetown University, Washington, DC 20016, USA

³ Department of Geology and Institute for Physical Science & Technology, University of Maryland, College Park, MD 20742, USA

Received 2008 May 15, accepted 2008 Jun 28

Published online 2008 Aug 30

Key words accretion disks – instabilities – magnetohydrodynamics (MHD) – turbulence

A Hopf bifurcation describes a transition from a steady state to an oscillatory one. This report describes how the presence of white Gaussian noise in the term driving the instability (the gain) affects the character of such a transition. We find that for small noise intensities the effective critical value of the bifurcation parameter increases linearly with the noise intensity. This result is used to quantitatively describe the onset of the magneto-rotational instability in a laboratory experiment using liquid metal with turbulent background flow.

Astron. Nachr. / AN 329, No. 7, 701–705 (2008) / DOI 10.1002/asna.200811012

Hopf bifurcations with fluctuating gain

S.A. Triana^{1,*}, D.H. Kelley¹, D. Zimmerman¹, D. Sisan², and D.P. Lathrop^{1,3}

¹ Department of Physics and Institute for Research in Electronics & Applied Physics, University of Maryland, College Park, MD 20742, USA

² Department of Physics, Georgetown University, Washington, DC 20016, USA

³ Department of Geology and Institute for Physical Science & Technology, University of Maryland, College Park, MD 20742, USA

Received 2008 May 15, accepted 2008 Jun 28

Published online 2008 Aug 30

Key words accretion disks – instabilities – magnetohydrodynamics (MHD) – turbulence

A Hopf bifurcation describes a transition from a steady state to an oscillatory one. This report describes how the presence of white Gaussian noise in the term driving the instability (the gain) affects the character of such a transition. We find that for small noise intensities the effective critical value of the bifurcation parameter increases linearly with the noise intensity. This result is used to quantitatively describe the onset of the magneto-rotational instability in a laboratory experiment using liquid metal with turbulent background flow.

© 2008 WILEY-VCH Verlag GmbH & Co. KGaA, Weinheim

1 Introduction

A real physical system is always subject to random fluctuations. This is particularly true in astrophysical and geophysical fluid dynamics where the presence of turbulence is unavoidable in most practical cases. Because systems exhibit transitions that are affected by turbulent fluctuations, it is relevant to understand, both qualitatively and quantitatively, the role of these turbulent fluctuations in the transition. Additive perturbations have been described in detail as a broadening or smoothing of the transition. If the gain in the dynamical system fluctuates, more exotic phenomena such as intermittent bursts (Sweet et al. 2001) may evolve in pitchfork bifurcations with multiplicative (amplification) noise. Examples of phenomena where the background base state is highly turbulent at instability onset include the magneto-rotational instability (MRI) as reported by Sisan et al. (2004) and the appearance of inertial waves in a rapidly rotating spherical-Couette apparatus (Kelley et al. 2007). Other examples include the gravity-wave bifurcation in a free-surface Taylor-Couette flow (Mujica & Lathrop 2006), surface switching of rotating fluid in a cylinder (Suzuki, Iima & Hayase 2006), and the well-known Belousov-Zhabotinsky reaction (Guderian 1996). Turbulent fluctuations are also studied in other kinds of instabilities like the dynamo (Laval et al. 2006; Leprovost & Dubrulle 2005). As many fluid and MHD instabilities arise from a (perhaps weakly) turbulent background state, this issue may be important in many natural settings. As the background state is the source of energy for the bifurcation, fluctuating backgrounds effect a fluctuating gain for the new state. The effect of random fluctuations on Hopf bifurcations has been

addressed in the past (Graham 1982) although the emphasis has been mathematical rather than physical. In this report we opt for a simplified mathematical description of the problem and apply it to a laboratory example.

A Hopf bifurcation describes the transition of a system from a steady to an oscillating state as a control parameter varies. Contained in the control parameter is information describing how the system will react to the external forcing. We will consider the turbulent background influencing the control parameter itself (see Pétrélis & Aumaître, 2006, and references therein).

Consider a dynamical system that has a single real control parameter μ and a single stable fixed point when $\mu < \mu_c$. A Hopf bifurcation occurs if by increasing μ past its critical value μ_c the fixed point loses stability and a limit cycle appears (Guckenheimer & Holmes 1983). Assuming $\mu_c = 0$ for simplicity, the normal form describing a Hopf bifurcation in polar coordinates is

$$\begin{aligned}\dot{r} &= \mu r + ar^3, \\ \dot{\theta} &= \omega + br^2,\end{aligned}\tag{1}$$

where r, θ represent the state of the system, a is the first Lyapunov exponent ($a < 0$ for a supercritical bifurcation), $\omega \neq 0$ and b is arbitrary. The steady state solution for the supercritical case $a = -1$ corresponds to oscillations with constant amplitude $r = \sqrt{\mu}$ and angular frequency ω . In the following sections we will study the effect of multiplicative noise on such a bifurcation model. Since we will be dealing with stochastic fluctuations, a statistical description is in order, i.e., a probability density enabling us to calculate averages will be found.

In Sects. 2 and 3 we will outline the technique used to find an appropriate probability density function. We will

* Corresponding author: triana@umd.edu

show analytically in Sect. 3 and numerically in Sect. 4 that the effective critical value of the bifurcation parameter increases linearly with noise strength for small noise intensities. Section 5 describes how the theory can be used using as an example a laboratory experiment displaying a Hopf bifurcation triggered by the MRI on a turbulent flow background.

2 Multiplicative noise

To study the influence of a fluctuating control parameter on the transition we write Eq. (1) as

$$\dot{r} = [\mu + \nu(t)]r + ar^3, \quad (2)$$

where $\nu(t)$ is the so-called Langevin force having the following properties:

$$\langle \nu(t) \rangle = 0, \quad \langle \nu(t)\nu(t') \rangle = q\delta(t-t'),$$

where $\langle \rangle$ denotes a time average and q is a positive number. The Langevin force $\nu(t)$ has therefore the properties of white Gaussian noise with strength q . This way of incorporating noise into the equations is called multiplicative because the noise term appears multiplying the dynamical variable r . Note that a noise term with zero mean as an extra *additive* term in Eq. (1) makes little physical sense unless r is allowed to have negative values. In such case Eq. (1) would describe then a *pitchfork* bifurcation. For sake of simplicity we will consider in the following *multiplicative* noise with zero mean only.

A general non-linear differential equation of one real variable ξ with multiplicative noise can be written as

$$\dot{\xi} = h(\xi, t) + g(\xi, t)\nu(t). \quad (3)$$

This is known as the *non-linear Langevin equation* (Risken 1996). The radial part of the (supercritical, $a = -1$) Hopf normal form with multiplicative noise (2) would then be a non-linear Langevin equation on the variable r with functions $h(r, t)$ and $g(r, t)$ defined as

$$h(r, t) = \mu r - r^3, \quad g(r, t) = r. \quad (4)$$

Our goal is to know the behavior of $\langle r \rangle$ as a function of both the control parameter μ and the noise strength q . For this purpose we will need a partial differential equation governing the probability density function for r , denoted $W(r, t)$, that corresponds to the dynamics described by the non-linear Langevin equation.

3 The Fokker-Planck equation

A partial differential equation for $W(r, t)$ using the *Stratonovich* interpretation (Stratonovich 1968) can be written as

$$\partial_t W(r, t) = \sum_{n=1}^{\infty} (-\partial_r)^n \left[D^{(n)}(r, t) W(r, t) \right],$$

where D^n are *Kramers-Moyal* coefficients and defined as (Kramers 1940; Moyal 1949)

$$D^{(n)}(r, t) = \frac{1}{n!} \lim_{\tau \rightarrow 0} \frac{\langle [\xi(t+\tau) - r]^n \rangle}{\tau} \Big|_{\xi(t)=r}.$$

Here $\xi(t+\tau)$ ($\tau > 0$) is a solution of Eq. (3) which at time t has the sharp value $\xi(t) = r$. This is known as the *Kramers-Moyal forward expansion* and if $D^{(n)}(r, t) = 0$ for $n \geq 3$ it is called the *Fokker-Planck* or *forward Kolmogorov* equation (Risken 1996). In the case of a non-linear Langevin equation it leads to a Fokker-Planck type equation

$$\partial_t W = -\partial_r \left[D^{(1)} W \right] + \partial_r^2 \left[D^{(2)} W \right].$$

The *stationary* solution (Risken 1996) for $W(r, t)$ is given by $W_{\text{st}}(r) = N e^{-\Phi(r)}$, where N is a normalization constant and $\Phi(r)$ is

$$\Phi(r) = \ln D^{(2)}(r) - \int^r \frac{D^{(1)}(r')}{D^{(2)}(r')} dr'.$$

The coefficients $D^{(1)}$ and $D^{(2)}$ are easily calculated:

$$D^{(1)}(r) = h(r) + g(r) \frac{dg(r)}{dr} \frac{q}{2},$$

$$D^{(2)}(r) = g^2(r) \frac{q}{2}.$$

Stated explicitly, the equation we want to solve is

$$\dot{r} = [\mu + \nu(t)]r - r^3, \quad (5)$$

and using Eq. (4) it is straightforward to show that the stationary probability density is

$$W_{\text{st}}(r) = 2 \frac{N}{q} r^{\frac{2\mu}{q}-1} \exp\left(\frac{-r^2}{q}\right), \quad (6)$$

where the normalization constant N is given by:

$$N = \frac{q^{1-\frac{\mu}{q}}}{\Gamma(\mu/q)}.$$

In the expression above $\Gamma(\mu/q)$ refers to the Gamma function. The ensemble average of r is then simply

$$\langle r \rangle = \int_0^{\infty} r W_{\text{st}}(r) dr = \sqrt{q} \frac{\Gamma(\frac{1}{2} + \frac{\mu}{q})}{\Gamma(\mu/q)}. \quad (7)$$

To see that this result reduces to the expected $\langle r \rangle \rightarrow \sqrt{\mu}$ when $q \rightarrow 0$ we note that the expression $\Gamma(J + \frac{1}{2})/\Gamma(J)$ can be written as an asymptotic series

$$\frac{\Gamma(J + \frac{1}{2})}{\Gamma(J)} = \sqrt{J} \left(1 - \frac{1}{8J} + \frac{1}{128J^2} + \dots \right). \quad (8)$$

Identifying J as μ/q the expression above clearly leads to the expected result when $J \gg 1$. If we keep terms up to first order in q/μ then we can write

$$\langle r \rangle^2 = \mu - \frac{q}{4}. \quad (9)$$

This tells us that for small amplitude fluctuations the bifurcation curve for $\langle r \rangle^2$ is essentially the same as in the case of a noise-free bifurcation, only shifted to the right an amount $q/4$. We will discuss the implications of this result in Sect. 5.

4 Numerical tests

The Langevin force is usually characterized by its *Power Spectral Density* $S(\omega)$ which can be calculated from the auto-correlation function $R(t)$ by using the Wiener-Khintchine Theorem:

$$\begin{aligned} R(t) &\equiv \langle \nu(t')\nu(t' - t) \rangle \\ &= \lim_{\tau \rightarrow \infty} \frac{1}{2\tau} \int_{-\tau}^{\tau} \nu(t')\nu(t' - t) dt' \\ &= q \delta(t) \\ S(\omega) &= \int_{-\infty}^{\infty} R(t)e^{-i\omega t} dt = q. \end{aligned}$$

When using discrete time sampling the correlation function $R(t)$ is defined only for discrete times. With a time interval T between samples we can define a function $R_T(t)$ defined for continuous t such that

$$\int_{-\infty}^{\infty} R_T(t) dt = \sum_{n=-\infty}^{\infty} R(nT)T.$$

A recipe for this is

$$R_T(t) \equiv T \sum_{n=-\infty}^{\infty} R(nT)\delta(t - nT).$$

The power spectral density $S(\omega)$ calculated from $R_T(t)$ is therefore

$$S(\omega) = T\sigma^2,$$

where σ is the standard deviation of the Gaussian noise.

We implemented numerical tests using a fourth-order Runge-Kutta integrator with fixed time step h . Noise was injected every n th step using a Gaussian random number generator with standard deviation σ . The resultant power spectral density is then

$$q = nh\sigma^2.$$

Data on Figs. 1 and 2 were produced using $h = 0.25$ and $n = 4$ with varying σ .

Figure 1 compares bifurcation curves calculated from Eq. (7) with numerical computation. The agreement is satisfactory. It can be seen that the sharp transition at the bifurcation becomes smoother as the noise intensity is increased. If turbulence can be modelled as white Gaussian noise, this implies that experiments with appreciable background turbulence will not exhibit a sharp transition to an oscillating state.

Also of interest is the spread of r after long times, i.e., the probability density W_{st} . Figure 2 compares the analytical result (6) to the probability density calculated from the numerical tests. As the noise intensity decreases, the probability density sharpens, eventually becoming a Dirac- δ for $q = 0$.

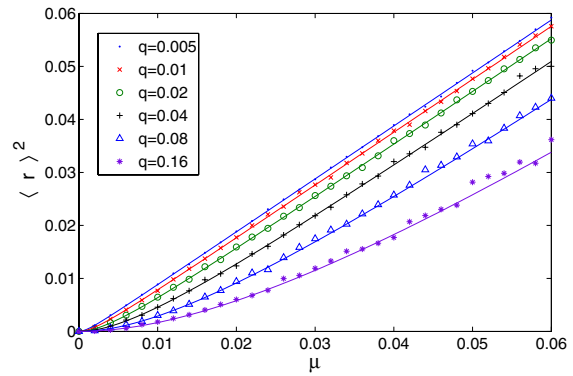


Fig. 1 (online colour at: www.an-journal.org) Squared average of r after 40 000 integration steps using a random initial condition between 0 and 0.1. The average was taken out of 5000 numerical runs, one for each random initial condition. Continuous lines are based on Eq. (7).

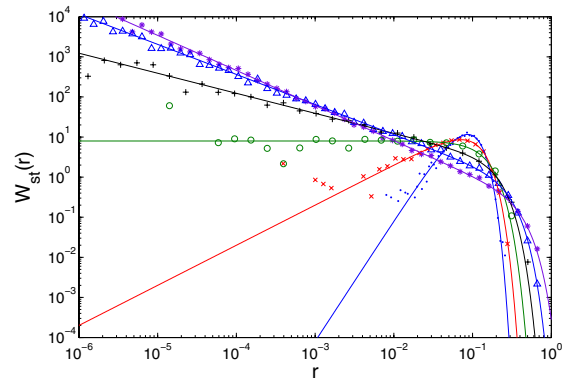


Fig. 2 (online colour at: www.an-journal.org) Stationary probability density $W_{st}(r)$ for $\mu = 0.01$ and different values of noise intensity. Continuous curves correspond to Eq. (6). Symbols and colors are the same as in Fig. 1.

5 The magneto-rotational instability

One hydromagnetic process that exhibits a Hopf type of bifurcation is the the magneto-rotational instability (MRI). It is of great importance in astrophysics where it gives a reasonable picture of the accretion mechanism in thin accretion disks, and considerable effort has been put forth to achieve the MRI in a laboratory experiment (Stefani et al. 2006). For a detailed description of the theory see Balbus & Hawley (1991).

The laboratory experiment performed by Sisan et al. (2004) to study the MRI is sketched in Fig. 3. In this setup, liquid metal (sodium) fills the space between an inner copper sphere and an outer spherical vessel. The inner sphere is able to rotate, and a uniform magnetic field is applied in the axial direction. An array of hall probes (oriented to measure magnetic fields in the cylindrical radial direction, thus avoiding saturation by the applied axial field) is just outside the spherical vessel to measure the field induced by the

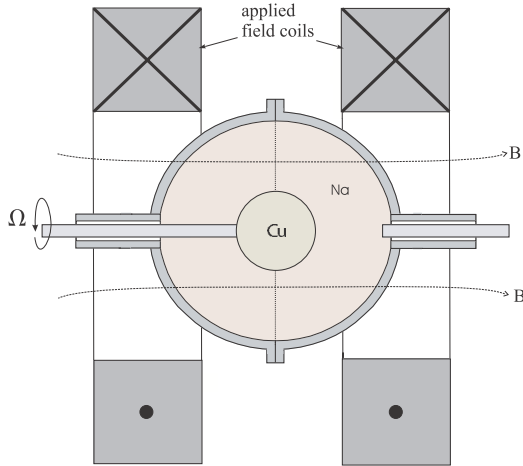


Fig. 3 (online colour at: www.an-journal.org) The 30 cm sodium experiment. A 10 cm diameter copper inner sphere immersed in liquid sodium is rotated as an external magnetic field (up to 0.2 T) is applied parallel to the rotation axis.

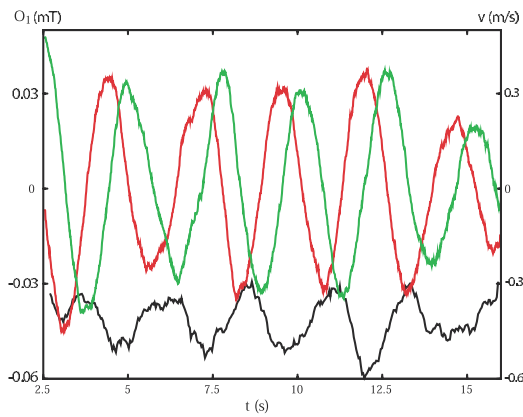


Fig. 4 (online colour at: www.an-journal.org) Time series of the Gauss coefficients of the O1 mode at a point on the spherical vessel. Red and green curves represent cos and sin components respectively. The velocity along a chord using ultrasound is shown in black.

flow. An ultrasound probe measures directly the flow along one chord.

The hydrodynamic Reynolds number for this setup is defined as $Re = \Omega ab/\nu$ where Ω is the rotation rate (in rad/s) of the inner sphere, $b = 5$ cm is the inner sphere radius, $a = 15.6$ cm is the spherical vessel radius and $\nu = 7.39 \times 10^{-3} \text{ cm}^2/\text{s}$ is the kinematic viscosity of sodium at 120°C . Other important dimensionless parameters are the magnetic Reynolds number, Rm , related to Re through

$$\eta Rm = \nu Re,$$

where $\eta \simeq 830 \text{ cm}^2/\text{s}$ is the magnetic diffusivity of sodium, and the Lundquist number

$$S = \frac{aB}{\eta\sqrt{\rho\mu_0}},$$

where B is the applied axial field intensity, $\rho = 0.927 \text{ g/cm}^3$ is the sodium density and $\mu_0 = 4\pi \times 10^{-7} \text{ N/A}^2$ is the per-

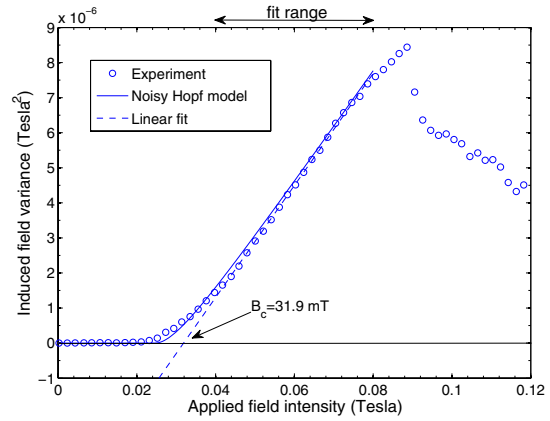


Fig. 5 (online colour at: www.an-journal.org) Variance of the experimentally observed oscillations in the magnetic field vs. the applied field intensity. The straight line is a linear fit with slope $s = 0.1598 \text{ mT}$. Continuous line is a noisy Hopf model with $q = 0.046$.

meability of free space. In the experiment $10^5 < Re < 10^7$, indicating that the flow is in a highly turbulent regime.

Sisan et al. (2004) found that when the inner sphere rotates at fixed Ω and the applied magnetic field is increased past some critical value B_c , oscillations are spontaneously excited in the coupled magnetic and velocity fields as evidenced by the hall probe array and ultrasound probe measurements shown in Fig. 4. The overall oscillation corresponds to a precessing pattern with azimuthal wave number $m = 1$. This mode is odd with respect to reflection about the origin and therefore labeled O1.

The threshold B_c depends on Ω defining bifurcation boundaries in the (B, Ω) parameter space or equivalently, in the (S, Rm) space as shown in Fig. 6. For a fixed rotation rate and starting from turbulent background the mode O1 appears when S is increased past the value defined by the bifurcation boundary.

The transition to an oscillatory state can be better studied at higher rotation rates ($Rm \sim 25$) where the induced field is stronger. A plot of the variance of the induced magnetic field (which is proportional to the squared oscillation amplitude when a definite mode dominates) as the applied magnetic field is varied is shown in Fig. 5. There is a linear trend from 45 mT to 80 mT as expected from a Hopf bifurcation model in which r represents the amplitude of the oscillating magnetic field. There is a deviation from an ideal Hopf normal form near the transition due to turbulent fluctuations in the fluid. The slope discontinuity one would expect in a noise-free Hopf bifurcation is absent; rather, the slope changes continuously, consistent with a noisy Hopf bifurcation model. For magnetic fields higher than 80 mT saturation effects take place and the Hopf approximation breaks down.

The results from Sect. 2 allow for a satisfactory description of the bifurcation near the transition. We establish first a critical B_c by the intersection of a linear fit with the hori-

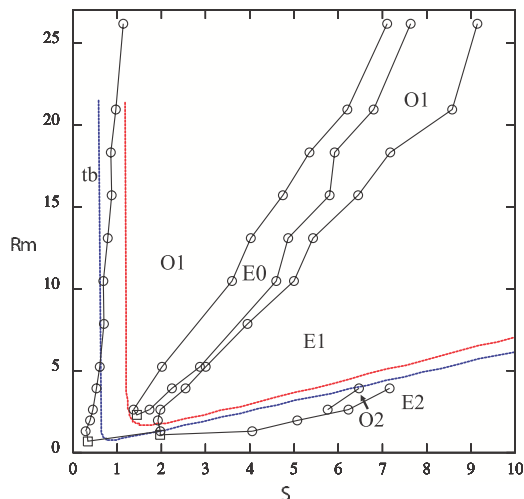


Fig. 6 (online colour at: www.an-journal.org) Phase diagram of the spontaneously excited states. Regions are defined by the mode with the largest oscillation amplitude. The states have regions associated with background turbulence (tb), mode O1 dominated, E0 dominated, followed by O1, E1, O2, and E2 modes. Also shown are theoretical stability boundaries for the longest wavelength (red) and second longest wavelength (blue) instabilities, calculated from the magneto-rotational dispersion relation.

zonal axis. This provides a quantitative definition for onset. In order to find the appropriate noise intensity q in Eq. (7) to fit the experimental data we need to use a properly scaled bifurcation parameter μ_{exp} defined by

$$\mu_{\text{exp}} \equiv s(B - B_c)\lambda,$$

where $s = 0.1598$ mT is the slope of the linear fit on the experimental data and λ is an arbitrary scaling factor. By setting $\lambda = 10\,000 \text{ T}^{-2}$ we map the horizontal axis in Fig. 5 to approximately the same range as in Fig. 1. The experimentally measured variance is to be accordingly scaled with the same factor λ . In this way the analytical and experimental data can be compared directly. Recalling Eq. (9), it is possible to define a linear fit to the family of analytical curves in Fig. 1. In analogy to the linear fit in Fig. 5, each linear fit will intersect the horizontal axis at $\mu_c = q/4$. Using a new variable $\mu_q \equiv \mu - \mu_c$ we can then find the analytical curve that best fits the data, yielding $q = 0.046$. We predict then that the critical parameter will increase linearly with q for small q/μ , or in other words, that the value of B_c needed for the MRI to set in will increase linearly with the magnetic Reynolds number R_m . In fact, this is precisely what is observed experimentally. Figure 6 shows that the primary O1 mode, starting from a fully turbulent background state, appears at a linearly increasing Lundquist number S with increasing R_m , a feature not predicted without noise fluctuations.

6 Discussion

The presence of fluctuations do not seem to alter the Hopf transition in a fundamental way. In fact we can say the MRI

induced bifurcations are robust under turbulent fluctuations as evidenced experimentally and suggested analytically by a noisy Hopf model. The presence of turbulence merely shifts the critical value of the bifurcation parameter. A turbulence-free system in the supercritical regime can be brought to a steady state with no oscillations by injecting an appropriate amount of noise. Since R_m is a measure of the turbulence present in the system, the fact that the experimentally measured critical curve for the primary instability deviates slightly from a vertical is consistent with the picture of turbulence-shifted criticality.

7 Summary

The effect of multiplicative noise on Hopf bifurcation was studied both analytically and numerically with consistent results. An experimental realization of a noisy Hopf bifurcation was described and the analytical results were used to describe experimental data. We showed that the MRI-induced transition from a steady to an oscillatory state with preexisting turbulent background can be both qualitatively and quantitatively be described by a Hopf bifurcation model with multiplicative noise. The model reproduces the smooth change in slope of the oscillation amplitude as the applied magnetic field is increased and also explains the linear growth of the critical Lundquist number S with increasing magnetic Reynolds number R_m .

References

- Balbus, S.A., Hawley, J.F.: 1991, *APJ* 376, 214
- Graham, R.L.: 1982, *Phys Rev A* 25, 6
- Guckenheimer, J., Holmes, P.: 1983, *Nonlinear Oscillations, Dynamical Systems, and Bifurcations of Vector Fields*, Springer
- Guderian, A., Dechert, G., Zeyer, K.P., Schneider, F.W.: 1996, *J Phys Chem* 100, 11
- Kelley, D.H., Triana, S.A., Zimmerman, D.S., Tilgner, A., Lathrop, D.P.: 2007, *GApFD* 101, 5
- Kramers, H.A.: 1940, *Phy* 7, 4
- Laval, J-P., Blaineau, P., Leprovost, N., Dubrulle, B., Daviaud, F.: 2006, *Phys Rev Lett* 96, 20
- Leprovost, N., Dubrulle, B.: 2005, *EPJB* 44, 3
- Moyal, J.E.: 1949, *JRSSD* 11
- Mujica, N., Lathrop, D.P.: 2006, *JFM* 551, 49
- Pétrélis, F., Aumaître, S.: *EFJB* 51, 3
- Risken, H.: 1996, *The Fokker-Planck Equation: Methods of Solution and Applications*, Springer
- Sisan, D.R., Mujica, N., Tillotson, W.A., Huang, Y.M., Dorland, W., Hassam, A.B., Antonsen, T.M., Lathrop, D.P.: 2004, *Phys Rev Lett* 93, 11
- Stefani, F., Gundrum, T., Gerbeth, G., Rüdiger, G., Schultz, M., Szklarski, J., Hollerbach, R.: 2006, *Phys Rev Lett* 97, 18
- Stratonovich, R.L.: 1968, *Conditional Markov Processes and Their Applications to Optimal Control*, Elsevier
- Suzuki, T., Iima, M., Hayase, Y.: 2006, *PhFl* 18, 101701
- Sweet, D., Ott, E., Finn, J.M., Antonsen, T.M., Lathrop, D.P.: 2001, *Phys Rev E* 63, 6